

NONDESTRUCTIVE EVALUATION OF METAL STRENGTH, TOUGHNESS, AND DUCTILITY THROUGH FRICTIONAL SLIDING

Steven Palkovic, Parth Patel, Soheil Safari, Simon C. Bellemare¹
Massachusetts Materials Technologies, LLC
Waltham, MA

ABSTRACT

Traditional assessment of mechanical properties requires the removal of a standardized specimen for destructive laboratory testing. A nondestructive in-situ method is a cost-effective and efficient solution for applications where sample cutouts are not feasible. This work describes developments in contact mechanics that use frictional sliding to evaluate the material strength and toughness of steel pressure vessels and pipelines.

Hardness, Strength, and Ductility (HSD) testing is a portable implementation of frictional sliding that provides a tensile stress-strain curve for assessment of the yield, ultimate tensile strength (UTS), and strain hardening exponent for power-law hardening metals. HSD testing incorporates four styluses of different geometry that generate grooves on the surface of a material as they travel. The measured geometry of these grooves along with the normal reaction forces on the stylus are correlated to representative tensile stress-strain values through finite element analysis (FEA) simulations. These principles have been extended to account for nonlinear strength behavior through the thickness of seam-welded steel pipes by using a combination of the HSD surface measurement, microstructure grain size, and chemistry. Frictional sliding tests are also used to assess material variation across a welded seam to identify different welding processes and the effectiveness of post-weld-heat-treatments (PWHT).

A second implementation of frictional sliding is Nondestructive Toughness Testing (NDTT), which provides an NDE solution for measuring fracture toughness by using a wedge-shaped stylus with an internal stretch passage to generate a Mode I tensile loading condition on the surface of a sample. The test produces a raised fractured surface whose height provides an indication of the materials ability to stretch near a propagating crack and is correlated to the crack-tip-opening-displacement (CTOD) measured from traditional laboratory

toughness testing. Experiments on pipeline steel indicate that NDTT can provide an index of fracture toughness to benchmark materials tested under similar conditions. Implementation of these new instruments to gather data for integrity management programs, fitness for service assessments, and quality control of new manufacturing will help to reduce risk and uncertainty in structural applications.

Keywords: Nondestructive, contact mechanics, strength, fracture toughness, condition assessment, quality control, material verification, integrity management.

INTRODUCTION

Engineers rely on material properties measured using standardized laboratory experiments to evaluate the capacity of structures, predict remaining life, and assess risk. Traditionally, these data have been obtained by extracting a sample of material from a larger component, machining the sample to the required specimen geometry, and then testing to failure using instrumented equipment. Examples include tensile tests for measuring the elastic-plastic behavior of metals to determine the yield strength, ultimate tensile strength (UTS), and strain hardening behavior. Another important mechanical test is the compact tension (CT) or single edge notched bend (SEB) for measuring fracture toughness properties that describe a material's resistance to the growth of an internal crack. These destructive tests are readily implemented during the fabrication of metal products, but can be expensive and disruptive for in-service infrastructure. Vintage assets may also have missing or incomplete documentation that do not provide all the necessary mechanical properties for modern integrity management programs. For these existing installations, nondestructive evaluation (NDE) methods can provide a direct non-invasive measurement of material properties. Recent developments have led to emerging NDE solutions that can provide accuracy and

¹ Contact author: s.bellemare@bymmt.com

reliability that is comparable to the traditional destructive benchmark [1-2].

This paper describes progress in two technologies that apply a technique known as frictional sliding to measure the material response in a shallow superficial groove on the material surface through contact mechanics. The measured nondestructive material response is used to predict the mechanical properties that would be measured through traditional destructive experiments on the same sample. The first methodology is Hardness, Strength, and Ductility (HSD) testing, which uses multiple spherical styluses to measure how metals respond to varying magnitudes of plastic deformation. This response can be used to predict the uniaxial stress-strain curve of steel, aluminum, copper, and nickel-based alloys [3-5]. A guiding system allows for testing circumferentially around the outer surface of pipe joints or pressure vessels to measure the mechanical properties of in-service pipelines [6]. An additional capability of HSD testing is to track changes in local properties, which can be used to assess the quality of welded connections [7]. The second approach is Nondestructive Toughness Testing (NDTT), which is a new method for measuring fracture toughness of ductile materials. A NDTT uses a wedge-shaped stylus to generate a shallow crack in a surface layer of material. The crack propagates in tension and generates a fractured ligament that experiments on pipeline steel have shown is correlated to the crack tip opening displacement (CTOD) measured with traditional laboratory tests [8].

For each technology, this paper describes the fundamental principles, provides validation data that compares the NDE measurement with destructive data on the same sample, and provides additional details for implementation on in-service pipelines or pressure vessels.

1. HARDNESS, STRENGTH, AND DUCTILITY (HSD)

1.1 Fundamentals of HSD Testing

HSD testing uses a portable implementation of the contact mechanics technique known as frictional sliding. During a frictional sliding test, a stylus indents a sample surface under a known load and then slides along the surface at a constant velocity to generate a permanent groove as shown schematically in Fig. 1. During a test, the normal force (P) and the width of the groove (a) are measured. The force and groove width are used to calculate the hardness with units of pressure given by,

$$H = \frac{8P}{\pi a^2} \quad (1)$$

where the projected contact area resisting the applied normal force is a semi-circle. The magnitude of deformation applied during the test is related to the attack angle (ϕ) that describes the relative angle between the stylus and the undeformed surface. For a spherical stylus, the attack angle varies based on the stylus radius (R), depth of penetration, and height of material pile-up

around the stylus. The attack angle can be calculated from the measured groove width and the known stylus radius with,

$$\phi = \frac{\pi}{2} - \cos^{-1}\left(\frac{a}{2R}\right). \quad (2)$$

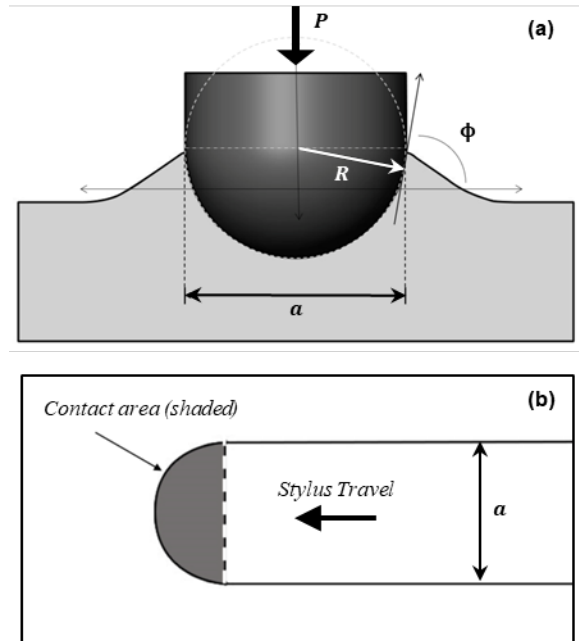


FIGURE 1: (a) SPHERICAL STYLUS ENGAGES WITH A SUBSTRATE UNDER LOAD. (b) STYLUS CREATES A RESIDUAL GROOVE AS IT TRAVELS ALONG SURFACE.

The measured hardness and attack angle are used to calculate a representative stress σ_r and representative strain ϵ_r . This concept relates the multiaxial stress state generated during a contact mechanics test with an equivalent uniaxial tension condition [9]. For a given attack angle, the representative strain is independent of the material flow properties, whereas the representative stress is a function of the elastic-plastic behavior [10]. This relationship can be established through FEA simulations of frictional sliding for a wide range of power-law hardening materials that are typical of engineering metals. The correlation between frictional sliding and tensile testing was first defined by Bellemare et al. for a conical stylus [3-5]. A similar approach was used to extend this analysis to spherical styluses, and the resulting functions are proprietary to Massachusetts Materials Technologies (MMT). HSD testing applies this concept by incorporating 4 styluses with different geometries to measure the material response at different locations along the uniaxial stress-strain curve. A complete uniaxial true stress (σ_t) versus true strain (ϵ_t) curve can then be obtained by performing a least-squares regression to the independent stylus measurements using Hollomon's equation [11],

$$\sigma_t = K\epsilon_t^n \quad (3)$$

where K is the material strength coefficient and n is the strain hardening exponent. Figure 2 shows the stress-strain curve after it is converted to engineering units to allow for the determination of the tensile strength properties with methods typically applied to the output of destructive tensile tests, including the 0.2% offset yield strength, 0.5% elongation under load (EUL) yield strength, and ultimate tensile strength (UTS).

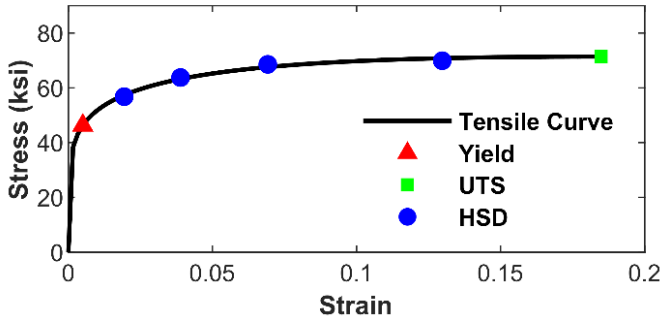


FIGURE 2: UNIAXIAL STRESS-STRAIN CURVE OBTAINED FROM σ_r - ϵ_r MEASUREMENTS AT 4 STYLUSES, AND THE RESULTING TENSILE PREDICTIONS. THE PLASTIC PORTION OF THE TENSILE CURVE IS OBTAINED BY FITTING TO THE HSD STYLUS MEASUREMENTS, AND THE ELASTIC PORTION IS SHOWN BY INTERSECTING A LINEAR LINE WITH A YOUNG'S MODULUS OF 29,000 KSI.

A portable unit for HSD testing is shown attached to a pipe joint in Fig. 3, and is currently configured to test flat surfaces or pipes ranging in size from 3 to 60 inches (7.6 to 150 cm) in diameter. The depth of each groove is less than 0.002 inches (51 μ m), allowing for the test to be considered as nondestructive for most engineering applications. Spring-loaded linear variable displacement transducers (LVDT) are used as profilometers to continuously measure the dimensions of the groove as the styluses slide across the sample surface. The load on each stylus is monitored with a calibrated force transducer. These measurements are used to calculate the frictional sliding hardness and attack angle using Eq. (1) and (2), respectively.

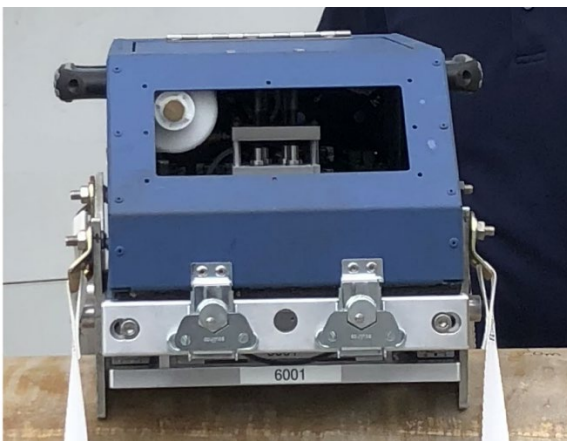


FIGURE 3: THE PORTABLE TESTER ATTACHES TO THE OUTER DIAMETER OF PIPE JOINTS, PRESSURE VESSELS, OR FITTINGS TO CONDUCT A CIRCUMFERENTIAL TEST.

The performance of this NDE measurement approach has been evaluated by comparing the HSD prediction with laboratory tensile tests for homogeneous samples like flat plate stock and seamless pipes. Results on 30 homogeneous samples are provided in Fig. 4 for both yield and UTS predictions. These data indicate a strong correlation and close agreement with the traditional benchmark for a wide range of steel grades and tensile behavior. Additional validation of this methodology has been obtained through testing on homogeneous aluminum materials [12]. Similar approaches using a single conical stylus was also used for testing brass and nickel-based alloys [5].

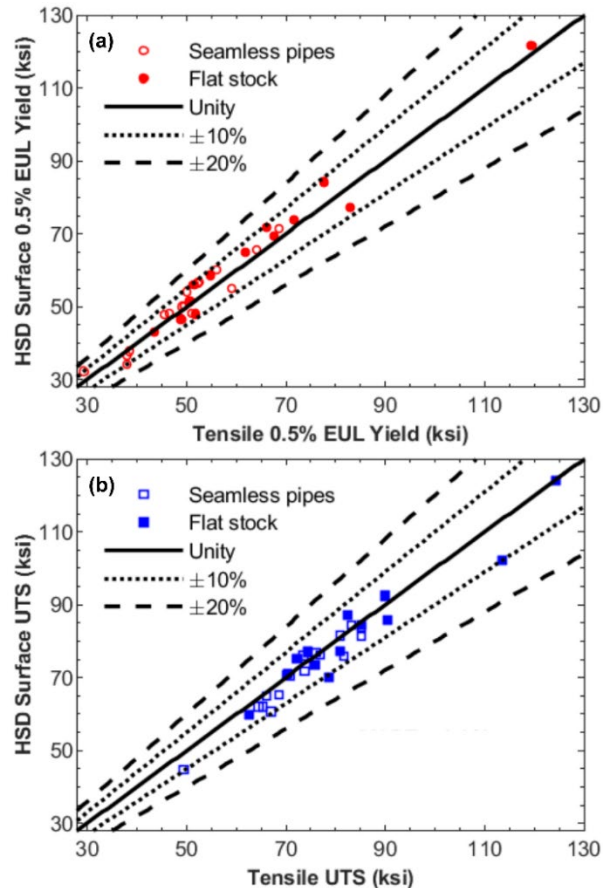


FIGURE 4: COMPARISON OF (a) YIELD AND (b) UTS PREDICTED WITH HSD TESTS AND MEASURED WITH TENSILE TESTS FOR 30 HOMOGENEOUS STEEL SAMPLES.

1.2 Measurement of Steel Pipeline Strength

NDE instruments like the HSD provide properties of surface material that is deformed during a test. This is an important consideration for longitudinal seam-welded pipe, where manufacturing processes induce an in-homogeneous distribution of material properties within the pipe wall. To investigate this effect, finite element analysis (FEA) was used to simulate changes in properties of a power-law hardening metal at different stages of manufacturing. A two-dimensional plane strain model was used to simulate cold forming a flat plate into a 12 inch (30.5

cm) diameter cylinder. The resulting deformed geometry and stress-strain field was used as the initial conditions for an axisymmetric model used to simulate radial expansion from an internal pressure. Figure 5 provides calculated yield strength values for finite elements through the thickness of the pipe wall at different stages of fabrication. Bending leads to a larger magnitude of strain hardening on the outer and inner surface of the pipe compared with material near the neutral axis that remains elastic. Application of a cold expansion or compression to meet dimensional tolerances homogenizes the distribution of strength properties due to the more uniform plastic strain field.

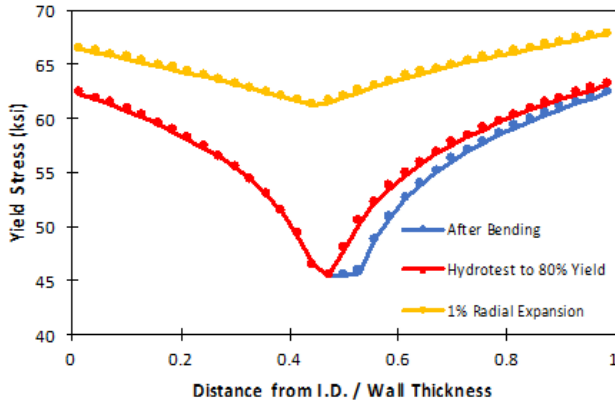


FIGURE 5: CALCULATED YIELD STRENGTH DISTRIBUTIONS THROUGH THE PIPE WALL AT DIFFERENT STAGES OF MANUFACTURING.

Experimental verification of the FEA results can be obtained by comparing HSD outer surface predictions with laboratory tensile tests on the same sample for seam-welded pipe joints. Tensile tests were performed in accordance with API 5L [13] using full-wall thickness coupons that provide effective properties based on the distribution of strength properties shown in Fig. 5. These test results are presented in Fig. 6 for 86 seam-welded samples with a unity plot that indicates the HSD surface predictions are on average 10% higher than the tensile measurement with a standard deviation of $\pm 9\%$. Additional verification of strength gradients through the wall thickness of seam-welded pipes has been obtained by comparing HSD measurements on the pipe outer surface with tests on the mid-wall material near the neutral axis that experiences the least strain hardening during bending. Differences in measured yield strength between the two surfaces for 6 seam-welded pipe joints ranged from -4.5% to $+20.6\%$ [14], which is comparable to differences with full-wall thickness coupons presented in Fig. 6.

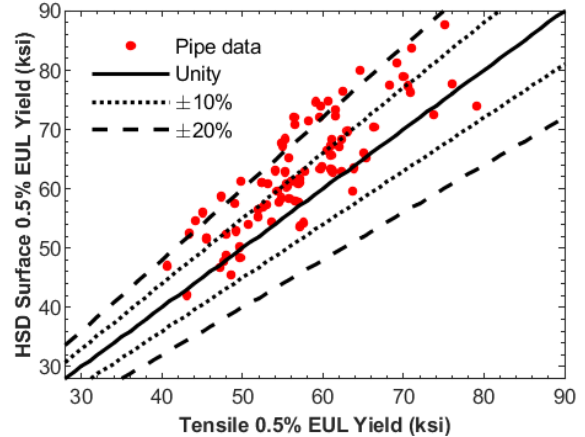


FIGURE 6: COMPARISON OF YIELD PREDICTED WITH HSD TESTS ON A SEAM-WELDED PIPE OUTER SURFACE AND MEASURED WITH FULL-WALL THICKNESS TENSILE COUPONS FOR 86 SEAM-WELDED SAMPLES.

To account for differences in strength properties of seam-welded pipes measured with HSD surface tests and full-wall thickness tensile coupons, additional NDE characteristics are considered. The HSD surface strength is combined with (1) the metallographic grain size evaluated with in-situ microscopy of the pipe surface microstructure, and (2) elemental composition from chemical analysis of steel shavings that are removed from the surface with a deburring tool. These parameters are integrated within a multiple linear regression model that ensures the most influential parameter is the HSD surface value, followed by the grain size that is correlated to strength through the well-known Hall-Petch relationship [15], and incorporates only the most statistically significant chemical elements. A comparison of the combined HSD predictions with results of laboratory tensile tests is presented in Fig. 7 for over 100 steel transmission pipe samples, including 17 seamless joints which consider only the surface HSD measurement. The population of pipe samples includes seamless, flash-welded (FW), electric-resistance-welded (ERW), and submerged-arc-welded (SAW) pipe joints covering a range of pipe vintages and steel grades. The mechanical properties for this database include 0.5% EUL yield strength spanning from 29 to 80 ksi (200 to 550 MPa), yield/UTS ratios ranging from 0.59 to 0.96, and strain hardening exponents ranging from 0.04 to 0.20.

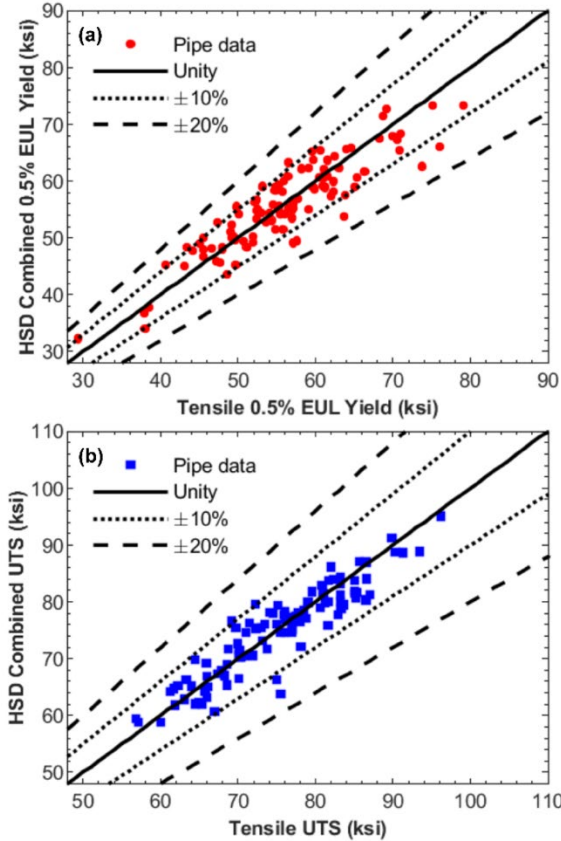


FIGURE 7: COMPARISON OF (a) YIELD AND (b) UTS PREDICTED WITH COMBINED HSD EQUATIONS AND MEASURED WITH TENSILE TESTS FOR OVER 100 STEEL TRANSMISSION PIPE SAMPLES.

The performance of this model has been assessed through blind testing on 50 pipe samples by a recent industry initiative sponsored through the Pipeline Research Council International (PRCI) [16]. The results presented in Fig. 7 include these results as well as additional pipe joints that have been tested since the completion of that program in the fall of 2017. A comparison of summary statistics for HSD testing and laboratory tensile tests based on the data shown in Figs. 4 and 7 are provided in Table 1 for both surface and combined prediction models.

TABLE 1: COMPARISONS OF HSD AND LABORATORY TENSILE TESTS MEASUREMENTS ON HOMOGENEOUS STEEL AND TRANSMISSION PIPE JOINTS

Summary statistic	Surface HSD & Homogeneous Tensile		Combined HSD & Steel Pipe Tensile	
	Yield	UTS	Yield	UTS
Root mean square error	3.1 ksi	3.5 ksi	3.4 ksi	3.1 ksi
Correlation coefficient	0.97	0.94	0.82	0.86

1.3 Evaluation of Weld PWHT

Frictional sliding allows for the continuous monitoring of changes in material properties as the stylus slides along the surface. As a result, HSD tests can be used to characterize local gradients in material properties where they exist, such as tests performed across a welded joint. The quality and reliability of a welded connection is significantly influenced by the application

of a post-weld-heat-treatment (PWHT) which can relieve residual stresses in the weld and normalize the microstructure by promoting recrystallization of material within the heat-affected-zones (HAZ). HSD tests can be performed across a weld to assess the effectiveness of PWHT by measuring relative changes in hardness which reflect changes in the local microstructure, chemistry, and internal stresses.

For transmission pipelines, ERW joints are produced by heating the opposing faces of a bent tube with an electrical current and then applying mechanical pressure to join the seam without the need for filler metal. Modern high frequency (HF) seams are subjected to a PWHT after forming and welding. HSD tests can be conducted circumferentially across the longitudinal seam to measure the material response across the HAZ near the weld. Representative HSD tests on HF welds are shown in Fig. 8 and display the broad range of hardness profiles that can be observed. The weld in Fig. 8(a) was likely not heated sufficiently resulting in multiple sharp hardness peaks that remain in the weld near the bondline and near the transitions to the surrounding base metal. Figure 8(b) shows a weld where a heat treatment was applied that led to significant hardening of the seam material which could decrease the toughness in the weld. Lastly, Fig. 8(c) shows a well-normalized seam that exhibits a decrease in hardness across the weld compared with the surrounding base metal.

To evaluate the effectiveness of a PWHT, the measured hardness in the base metal that is unaffected from the welding process is compared to the heat-affected regions near the seam. To compare pipes, the normalized relative change in hardness can be calculated using,

$$\Delta H = (H_{HAZ} - H_{BM})/H_{BM} \quad (4)$$

where H_{HAZ} is the average hardness of the identified HAZ near the seam, and H_{BM} is the average hardness of the base metal surrounding the HAZ. In the examples shown on Fig. 8, the HAZ is shaded yellow whereas the base metal is not shaded. Figure 9 shows a histogram of the calculated ΔH for 36 HF pipe joints. The data show a bimodal distribution, with one peak centered at $\Delta H = +15\%$ that is associated with welds like Fig. 8(a) that were not effectively normalized. The second peak has a much broader distribution and is centered near $\Delta H = 0\%$, which is attributed to normalized welds like Fig. 8(c) with varying degrees of effectiveness. One HF weld exhibited a significant hardness increase of $\Delta H = +30\%$ which is shown in Fig. 8(b), and is likely due to an improper PWHT.

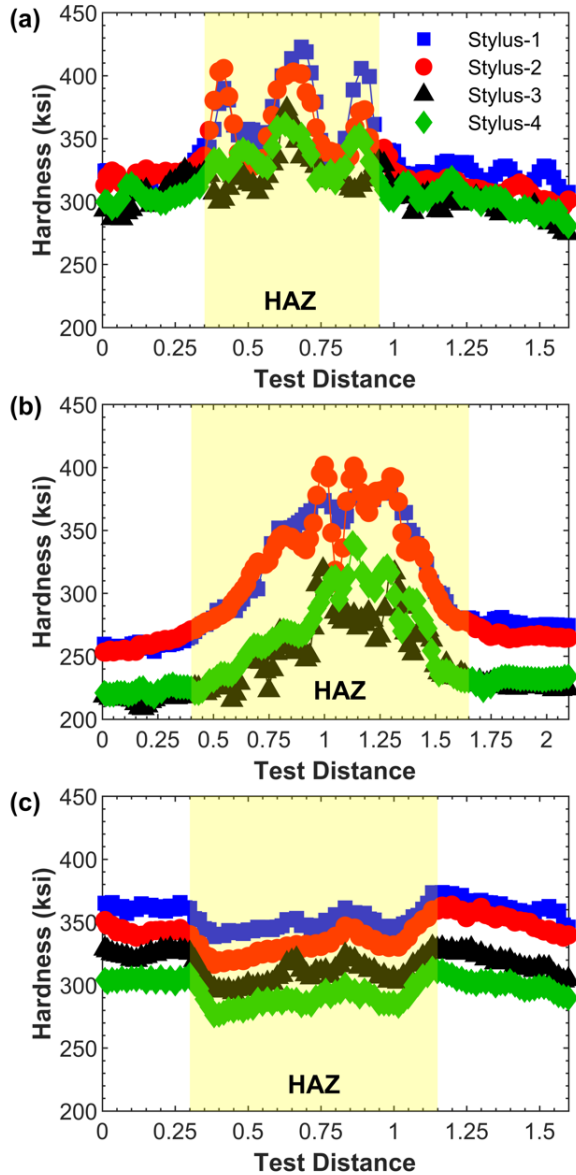


FIGURE 8: HSD TESTS PERFORMED ACROSS HF-ERW SEAMS. EXAMPLES OF A WELD (a) NOT NORMALIZED, (b) HARDENED, AND (c) NORMALIZED.

Other applications of HSD tests across the weld include prediction of filler weld metal strength properties, and classification of different ERW welding processes to differentiate between older low frequency (LF) and more modern HF seams [17]. These capabilities provide unique information for quality control of the mechanical response in welded joints and condition assessment of existing assets with incomplete or missing documentation.

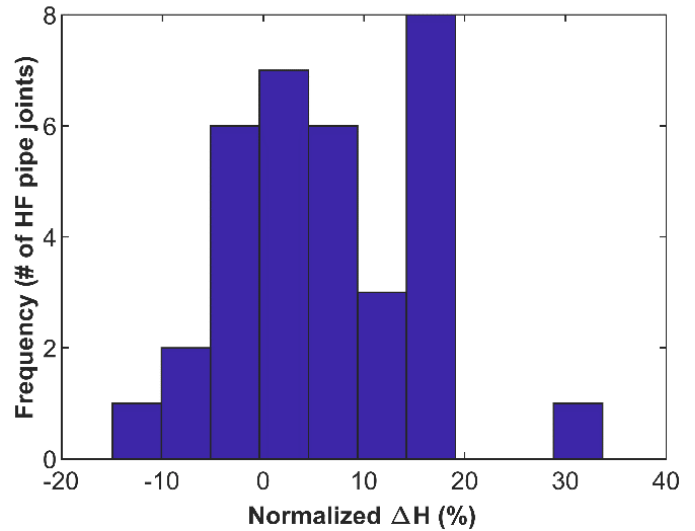


FIGURE 9: HISTOGRAM SHOWING THE FREQUENCY OF NORMALIZED HARDNESS CHANGES (ΔH) ACROSS THE WELDED SEAM FOR 36 HF-ERW PIPES.

2 NONDESTRUCTIVE TOUGHNESS TESTING

2.1 Fundamentals of NDTT

NDTT is a new concept for measuring the material response near a crack that is loaded in tension and propagates parallel to the material surface. An overview of NDTT mechanics is shown in Fig. 10. The NDTT stylus is a wedge with an opening along the upstream face called the stretch passage. Material entering the stretch passage is subjected to a tensile stretch as the surrounding substrate separates into a chip and flows up the inclined-face of the cutting tool. After enough deformation the material within the stretch passage fractures, resulting in a raised ligament of material that remains on both the cut surface of the substrate and the opposing face of the chip.

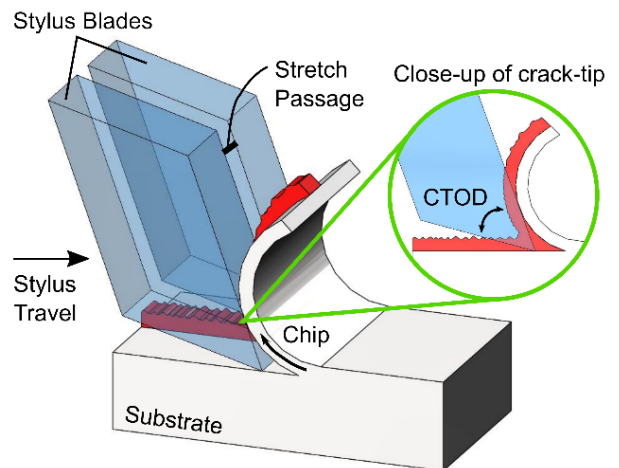


FIGURE 10: INTERACTION OF THE NDTT STYLUS WITH A METALLIC SUBSTRATE TO GENERATE A FRACTURED LIGAMENT, SHOWN IN RED.

2.2 NDTT Prototype and Test Procedures

The current NDTT prototype is shown in Fig. 11. The desktop unit consists of a stiff frame with an attached stepper motor that provides translational movement to an assembly that hosts the NDTT stylus. This assembly consists of an angled block that sets the cutting angle of the blades with respect to the surface of the test sample. The stylus fixture is attached to the angle block and uses multiple set screws to secure the stylus during a test. The NDTT stylus is composed of two hardened tool steel blades that are separated by a shim which creates an opening that functions as the stretch passage during testing. The test sample is fixtured to the NDTT frame in the desired test orientation using a clamping mechanism.

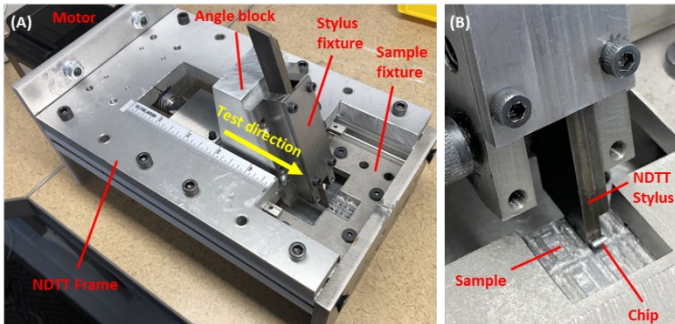


FIGURE 11: (a) OVERVIEW OF THE NDTT UNIT. (b) CLOSE-UP OF THE STYLUS ENGAGING WITH A TEST SAMPLE.

During a test, the NDTT stylus is held at a constant rake angle, which controls the amount of cutting force required and proportion of tensile and shear force applied to the test sample. The stretch passage width sets the volume of material which will fracture during an experiment. A larger stretch passage width requires a deeper penetration depth to ensure the fractured ligament will form. A cutting lubricant is applied during testing to reduce friction, lower the necessary cutting force, and reduce the wear rate of the stylus.

After testing, the geometry of the fractured ligament is measured with a contact profilometer using a spring-loaded linear variable displacement transducer (LVDT). The profilometer rasters across the fractured ligament in the direction of the cut-width. The profilometer output from a typical scan is shown in Fig. 12. These data are processed to (1) identify the cut surfaces on either side of the fractured ligament, (2) select a region of the cut surface to rotate the scan and find an averaged elevation of each blade, (3) calculate the relative height between the cut surface and the peak of the fractured ligament on both sides of the ligament (δ_l, δ_r), and (4) calculate the average ligament height (δ_L) for comparison with laboratory CTOD (δ_I) measurements using,

$$\delta_L = (\delta_l + \delta_r)/2 \quad (5)$$

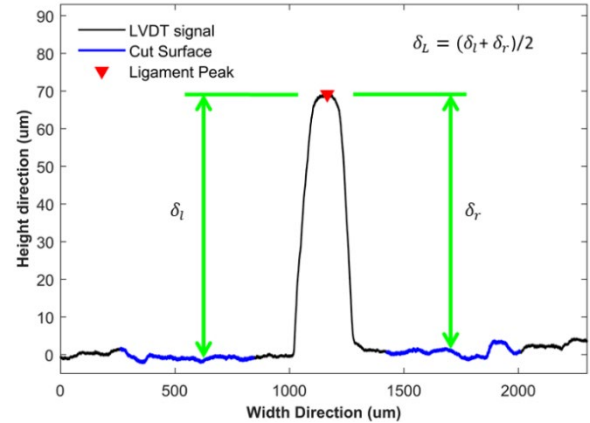


FIGURE 12: TYPICAL SCAN OF THE FRACTURED LIGAMENT AND CUT SURFACE

2.3 Fracture Surface Observations

A Scanning Electron Microscope (SEM) was used to examine the features of the fractured ligaments. A representative test section is shown in Fig. 13, with several higher magnification images of the raised fracture surface exhibiting evidence of ductile fracture such as microvoids and micrometer-sized dimples. Prior experiments on multiple steel pipeline grades have found that the height of the fractured ligament with respect to the cut surface provides an indication of the magnitude of tensile stretch the material can withstand at failure. The fractured ligament height was found to be correlated to the CTOD measured with traditional destructive laboratory experiments on the same sample [6].

2.4 Future Developments

The NDTT method is still a new and developing approach which requires further study to provide a more complete understanding of how it measures the material fracture response. The stretch passage width is on the order of 0.003 inches (76 μm), meaning that for most vintage pipeline steels, less than 5 grains of the microstructure are being included across the width of fracture surface. This small volume can constrain the ability of an advancing crack to propagate compared to larger-scale experiments. An increase in the stretch passage width requires a corresponding increase in cutting depth to ensure that the portion of the separated chip spanning across the stretch passage is thick enough to withstand the cutting forces without failing. If material in this region fails, two separate chips are formed, and no fractured ligament is created. These related constraints on stretch passage geometry, penetration depth, and cutting force will be mapped out through future testing on metallic materials.

Additional parameters that will be further studied include the rake angle that defines the relative angle between the cutting blade and sample surface. From trigonometry, a larger rake angle will provide a larger proportion of upwards tensile force compared to horizontal cutting force which could influence the material response. Another important parameter is the penetration depth which can change the magnitude of plastic deformation in the chip and lead to a transition from elastic-

plastic bending for shallow depths to plastic shearing at larger depths [18]. For the range of depths considered in prior testing, elastic-plastic bending was observed for all tests, but the response may change when larger depths are considered.

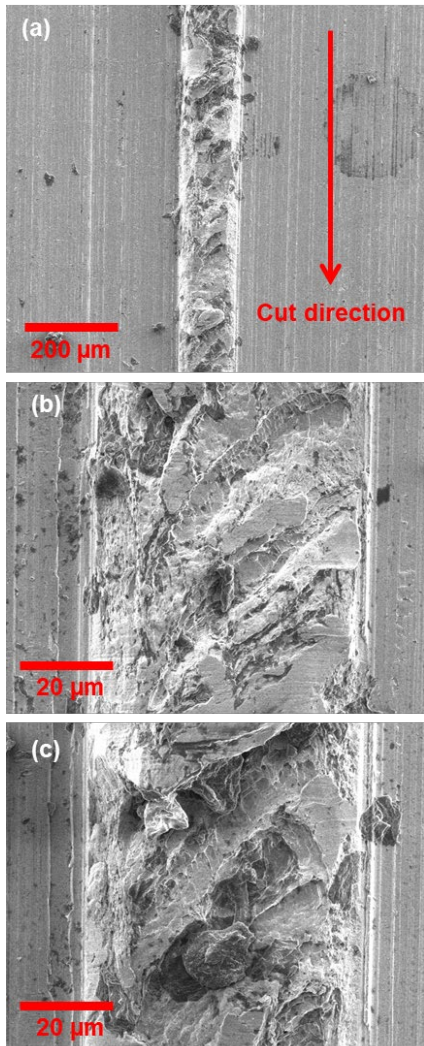


FIGURE 13: SEM OF THE FRACTURED LIGAMENT. (a) OVERVIEW IMAGE OF 1 MM LONG SECTION OF TEST. (b-c) CLOSE-UP OF FRACTURE SURFACE.

The design of the next NDTT unit will incorporate several features to allow for testing on curved surfaces like the outer diameter of a pipe joint. This will require the alignment of the stylus with the surrounding surface as it travels. These concepts are similar to methods already implemented by HSD equipment, which uses a surface referencing system that contacts the undeformed surface at multiple locations outside the test location to self-align as the unit tests circumferentially around a pipe.

CONCLUSIONS

This paper provides an overview of new developments for two NDE methods that are capable of measuring mechanical properties of in-service pipelines and pressure vessels. Through

the research and field applications completed, the following is concluded:

- HSD testing can accurately predict the tensile yield and UTS of homogeneous power-law hardening metals. For applications where a gradient in mechanical properties exists through the thickness, such as seam-welded pipe joints that have been cold worked during fabrication, HSD predictions can be combined with additional NDE measurements to develop predictive models that can be compared with traditional full-wall thickness tensile coupons. The performance of these combined methods has been assessed through internal testing and external blind validation programs on over 100 steel transmission pipe joints.
- HSD tests performed across a welded joint provide information on local changes in mechanical properties. This capability has been applied to measure the effectiveness of PWHT for ERW longitudinal seams by quantifying the magnitude of any hardness variations in the seam through normalization of the microstructure.
- NDTT is an emerging technique for measuring how ductile metals respond to a propagating crack loaded in tension that is constrained to a shallow surface layer of material. Experiments on pipeline steels have shown evidence of ductile fracture behavior and correlations with traditional laboratory fracture toughness measurements. Future efforts will study the influence of test parameters on the measured material responses.

ACKNOWLEDGEMENTS

Massachusetts Materials Technologies (MMT) acknowledges financial support provided from the National Science Foundation (NSF) Small Business Innovation Research (SBIR) program, Army Research Office (ARO), and MassVentures SBIR Targeted Technologies (START) Program, as well as TransCanada Pipelines and NOVA Chemicals.

REFERENCES

- [1] F.M. Haggag, "In-situ measurements of mechanical properties using novel automated ball indentation systems," Small Specimen Test Techniques Applied to Nuclear Reactor Vessel Thermal Annealing and Plant Life Extension, ASTM STP 1204, W. R. Corwin F. M. Haggag, and W. L. Server, Eds., ASTM, Philadelphia, 1993.
- [2] S.D. Palkovic, K. Taniguchi and S.C. Bellemare, "Nondestructive evaluation for yield strength and toughness of steel pipelines," CORROSION 2018, NACE International, 2018.
- [3] S.C. Bellemare, M. Dao and S. Suresh, "The frictional sliding response of elasto-plastic materials in contact with a conical indenter," International Journal of Solids and Structures, 44(6), 2007.
- [4] S.C. Bellemare, M. Dao and S. Suresh, "Effects of mechanical properties and surface friction on elasto-plastic sliding contact," Mechanics of Materials, 40, 2008.

- [5] S.C. Bellemare, M. Dao and S. Suresh, "A new method for evaluating the plastic properties of materials through instrumented frictional sliding tests," *Acta Materialia*, 58, 2010.
- [6] S.D. Palkovic, K. Taniguchi and S.C. Bellemare, "In-Ditch Materials Verification Methods and Equipment for Steel Strength and Toughness," *Pipeline Pigging and Integrity Management*, Houston, TX, 2018.
- [7] S.D. Palkovic, B.M. Willey, M.J. Tarkanian, S.C. Bellemare, "Measuring variations in mechanical properties across an electric-resistance-welded (ERW) pipe seam with a portable device," *Journal of Pipeline Engineering*, 2015.
- [8] S.D. Palkovic, S.C. Bellemare, K.K. Botros, X.D. Chen, R. Kania, "Calibration of a nondestructive toughness tester (NDTT) for measuring fracture toughness properties of pipeline steel," *IPC 2018*.
- [9] A.G. Atkins and D. Tabor, "Plastic indentation in metals with cones," *Journal of the Mechanics and Physics of Solids*, 1965.
- [10] N. Ogasawara, N. Chiba and X. Chen, "Representative strain of indentation analysis," *Journal of Materials Research*, 2005.
- [11] J.H. Hollomon, "Tensile deformation," *Aime Trans.*, 1945.
- [12] S.D. Palkovic, B. Willey, S.S. Loaliyan, S.C. Bellemare, "Application of Frictional Sliding to Evaluate the Strength, Ductility and Toughness of Cold Spray Coatings," 2018.
- [13] American Petroleum Institute, "API 5L Specification for Line Pipe," 2004.
- [14] S.C. Bellemare, S.D. Palkovic and K. Taniguchi, "Hardness, Strength, and Ductility (HSD) Testing of Line Pipes: Initial Validation Testing (Phase 1)," NDE-4-4 Catalog No. PR-610-163756-R01, Apr 2017.
- [15] E.O. Hall, "The deformation and ageing of mild steel: III Discussion of Results," *Proceedings of the Physical Society, Section B*, 1951.
- [16] S.D. Palkovic, K. Taniguchi and S.C. Bellemare, "Hardness, Strength, and Ductility (HSD) Testing of Steel Pipelines for Tensile Strength Properties," NDE 4-8 Catalog No. CWA-17-001.MMT, Nov 2018.
- [17] S.D. Palkovic, P. Patel, S.S. Loaliyan, M. Islam, S.C. Bellemare, "Nondestructive classification of LF, HF, and HF-normalized ERW longitudinal seam," *Pipeline Pigging and Integrity Management*, Houston, TX, 2019.
- [18] T. Atkins, *The Science and Engineering of Cutting*, Elsevier Ltd., 2009.